



21 **What is already known on this topic**

- 22 ● Many infectious diseases present an environmental pattern in their incidence.
- 23 ● Environmental factors, such as climate and weather condition, could drive the space and time  
24 correlations of infectious diseases, including influenza.
- 25 ● Severe acute respiratory syndrome coronavirus 2 (SARS-CoV-2) can be transmitted through  
26 aerosols, large droplets, or direct contact with secretions (or fomites) as influenza virus can.
- 27 ● Little is known about environmental pattern in COVID-19 incidence.

28 **What this study adds**

- 29 ● The significant association between COVID-19 daily incidence and temperature was  
30 confirmed, using 3 methods, based on the data on COVID-19 and weather from 31  
31 provincial-level regions in mainland China.
- 32 ● Environmental factors were considered on the basis of SEIR model, and a modified  
33 susceptible-exposed-infectious-recovered (M-SEIR) model was developed.
- 34 ● Simulations of the COVID-19 outbreak in Wuhan presented similar effects of temperature on  
35 incidence as the incidence decrease with the increase of temperature.

36 **ABSTRACT**

37 **OBJECTIVE**

38 To investigate the impact of temperature and absolute humidity on the coronavirus disease 2019  
39 (COVID-19) outbreak.

40 **DESIGN**

41 Ecological study.

42 **SETTING**

43 31 provincial-level regions in mainland China.

44 **MAIN OUTCOME MEASURES**

45 Data on COVID-19 incidence and climate between Jan 20 and Feb 29, 2020.

46 **RESULTS**

47 The number of new confirm COVID-19 cases in mainland China peaked on Feb 1, 2020. COVID-19  
48 daily incidence were lowest at -10 °C and highest at 10 °C, while the maximum incidence was  
49 observed at the absolute humidity of approximately 7 g/m<sup>3</sup>. COVID-19 incidence changed with  
50 temperature as daily incidence decreased when the temperature rose. No significant association  
51 between COVID-19 incidence and absolute humidity was observed in distributed lag nonlinear models.  
52 Additionally, A modified susceptible-exposed-infectious-recovered (M-SEIR) model confirmed that  
53 transmission rate decreased with the increase of temperature, leading to further decrease of infection  
54 rate and outbreak scale.

55 **CONCLUSION**

56 Temperature is an environmental driver of the COVID-19 outbreak in China. Lower and higher  
57 temperatures might be positive to decrease the COVID-19 incidence. M-SEIR models help to better  
58 evaluate environmental and social impacts on COVID-19.

59

60 **Keywords:** COVID-19, Temperature, Humidity, Dynamic transmission model.

61

## 62 INTRODUCTION

63 In December 2019, an outbreak of novel coronavirus pneumonia occurred in Wuhan, Hubei Province,  
64 China, and then were declared as an international public health emergency by the World Health  
65 Organization (WHO) on January 30 2020. The disease was officially named as coronavirus disease  
66 2019 (COVID-19) and the newly emerged virus was named as SARS-CoV-2 in February 2020.<sup>1</sup>

67 Previous studies on early cases showed that the disease severity of COVID-19 with a 2.3%  
68 case-fatality rate,<sup>2</sup> is much lower than Middle East Respiratory Syndrome (MERS) and Severe Acute  
69 Respiratory Syndrome (SARS).<sup>3</sup> However, as Li et al. reported,<sup>4</sup> the number of COVID-19 cases  
70 doubled every 7.4 days between December 2019 and January 2020, indicating COVID-19 might be  
71 more infectious than SARS and MERS. In March 2020, the outbreak of COVID-19 was declared as a  
72 global pandemic for the coronavirus rapidly expanded throughout China and to 116 other countries and  
73 territories worldwide.

74 Many infectious diseases present an environmental pattern in their incidence. A few studies on  
75 environmental issues, such as climate and weather condition, indicated that environmental factor could  
76 drive the space and time correlations of infectious diseases.<sup>5-7</sup> Based on analysis on climate predictors,  
77 James D et al. found that humidity and temperature are optimal indicators in predicting influenza  
78 epidemics in tropical regions.<sup>8</sup> Temperate regions of the Northern and Southern Hemispheres are  
79 characterized by highly synchronized annual influenza circulations during their winter months  
80 respectively.<sup>5,7,8</sup> In the United States, an epidemiological study indicated that lower specific humidity  
81 is related to the occurrence of pandemic influenza, which is consistent with earlier finding in laboratory  
82 experiments.<sup>9</sup> Absolute humidity, the actual mass of water vapor, is identified as a main cause of

83 seasonal influenza epidemics.<sup>10</sup> The influenza presents significant seasonal fluctuation in temperate  
84 monsoon climate regions as the absolute humidity varies greatly in summer and winter, which could  
85 help the multiplication of virus.

86 Severe acute respiratory syndrome coronavirus 2 (SARS-CoV-2) can be transmitted through  
87 aerosols, large droplets, or direct contact with secretions (or fomites) as influenza virus can.<sup>11</sup> However,  
88 the environmental pattern remains to be elucidated in COVID-19 incidence. Based on dynamical  
89 equations, susceptible-exposed-infectious-recovered (SEIR) modeling has been developed and used to  
90 estimate key epidemic parameter to better characterize mechanism for the epidemic dynamics.<sup>12-14</sup>  
91 Therefore, we explored the association between daily incidence and climate conditions using locally  
92 weighted regression and smoothing scatterplot (LOESS) and distributed lag nonlinear models (DLNMs)  
93 based on the data on COVID-19 and weather from 31 provincial-level regions in mainland China,  
94 between Jan 20 and Feb 29, 2020. Furthermore, we took account of environmental factors on the basis  
95 of SEIR model, and developed a modified susceptible-exposed-infectious-recovered (M-SEIR) model  
96 to characterize the climate impacts on epidemic dynamics.

97

## 98 **METHODS**

### 99 **Study data**

100 Data on COVID-19, including the number of new confirmed and probable cases were obtained from  
101 the China National Health Commission (CNHC) using the CoV2019 package<sup>15</sup>  
102 (<http://www.nhc.gov.cn/>). COVID-19 data were collected among all of the 31 provincial-level regions  
103 in mainland China and Wuhan city, between Jan 20 and Feb 29, 2020. COVID-19 emerged in Wuhan

104 city at the end of 2019 and rapidly spread across mainland China. Thus, population dynamic factors,  
105 including birth rate and death rate, were not considered here. Finally, daily incidences among the 31  
106 provincial-level regions and Wuhan city were calculated by dividing the number of new confirmed  
107 cases by the population size at the end of 2018 respectively, and was reported per 100,000 population.

108 Daily temperatures (T) and relative humidity (RH) of 344 cities of the corresponding period were  
109 collected from the meteorological authority in mainland China. Means of temperatures and absolute  
110 humidity were further calculated for every provincial-level region. The Clausius-Clapeyron relation  
111 equation was used to calculate absolute humidity (AH) as following:

$$112 \quad AH = \frac{6.112 \times e^{\frac{17.67T}{T+243.5}} \times RH \times 2.1674}{273.15 + T}$$

113 Data on climate conditions and population were retrieved from official reports previously released  
114 in mainland China. Therefore, the ethical review was not required.

### 115 **Statistical analysis**

116 Trends of climate factors and daily COVID-19 incidence indicators, including the incidence and the  
117 common logarithm of numbers of newly confirmed cases (lgN), were analyzed with locally weighted  
118 regression and smoothing scatterplot (LOESS) in 31 provincial-level regions in mainland China from  
119 Jan 20 to Feb 29, 2020.

120 Developed on the definition of a cross-basis, DLNMs were used to infer the  
121 exposure-lag-response associations between climate factors and daily confirmed cases of COVID-19.  
122 DLNMs were constructed for mainland China outside of Hubei Province, Hubei Province outside of  
123 Wuhan city, and Wuhan city respectively. To induce the redundant analysis, temperature and absolute

124 humidity of mainland China were represented by data on the capital, Beijing. Additionally, temperature  
125 and absolute humidity means of the sites in Hubei Province outside of Wuhan, were calculated as a  
126 representative of Hubei Province data.

127 To better understand the potential environmental driver of COVID-19, we took account of  
128 environmental factors on the basis of SEIR model and constructed the M-SEIR model to simulate the  
129 COVID-19 outbreak dynamic in Wuhan after travel restriction was put into force. Further sensitivity  
130 analysis was performed for quantitative risk assessment to evaluate the relationships between  
131 environmental parameter and COVID-19 incidence.

132 The equations of M-SEIR model were given in the following:

$$\begin{aligned}\frac{dS(t)}{dt} &= \frac{-\beta_t S(t)I(t)}{N} \\ \frac{dE(t)}{dt} &= \frac{\beta_t S(t)I(t)}{N} - \sigma E(t) \\ \frac{dI(t)}{dt} &= \sigma E(t) - \gamma I(t) \\ \frac{dR(t)}{dt} &= \gamma I(t) \\ \beta_t &= \beta_1(1 + \beta_2 AH + \beta_3 T)\end{aligned}$$

133 where  $S(t)$ ,  $E(t)$ ,  $I(t)$ , and  $R(t)$  were the number of susceptible, exposed, infectious, and removed  
134 individuals at time  $t$ ;  $\frac{1}{\sigma}$  and  $\frac{1}{\gamma}$  were the mean latent and infectious period;  $\beta_t$  was a time dependent  
135 rate of infectious contact;  $\beta_1, \beta_2$  and  $\beta_3$  were constant coefficients.

136 The simulations of COVID-19 dynamic and sensitivity analysis were conducted by using the  
137 system dynamic section in AnyLogic software (version 8.5.2). The specific depict of parameter values

138 in modified model and basic model details were included in **Supplementary Table 1**.

139

## 140 **RESULTS**

141 80,981 cases of COVID-19 (cases of decrease in accounting not removed) was confirmed in 31  
142 provincial-level regions in mainland China, between Jan 20 and Feb 29, 2020. Out of 80,981 cases,  
143 68,034 (84.01%) were diagnosed in Hubei Province. Daily number of new confirmed cases and daily  
144 incidence in mainland China were presented in **Figure 1** and **Supplementary Table 1**. Daily number of  
145 cases peaked on Feb 12 and then it decreased, due to the adjustment in the diagnostic criteria of Hubei  
146 Province. And the number of cases and the incidence in China (outside of Hubei Province) have begun  
147 to decline early in Feb.

148 From Jan 20 to Feb 29, 2020, temperature and absolute humidity varied in 31 provincial-level  
149 regions in mainland China (**Figure 2**). The highest temperature (26 °C) and absolute humidity (19.45  
150 g/m<sup>3</sup>) were observed in Hainan Province and the lowest temperature (-22 °C) and absolute humidity  
151 (0.54 g/m<sup>3</sup>) were observed in Jilin Province, which resulted from the geographical location. COVID-19  
152 daily incidence indicators (daily incidence and lgN) increased as the absolute humidity rose and  
153 declined slightly when absolute humidity reached approximately 7 g/m<sup>3</sup> (**Figure 3**). Analysis for Hubei  
154 Province (outside of Wuhan) and Wuhan showed highly similar results (**Supplementary Figure 1 and**  
155 **Supplementary Figure 2**). Differences lay in the fact that cases clinically diagnosed without nucleic  
156 acid testing had been counted as confirmed cases in Hubei Province since Feb 12, which might increase  
157 potential bias in the model.

158 Associations between temperature and COVID-19 relative risk (RR) in mainland China (outside

159 of Hubei Province), Hubei Province (outside of Wuhan) and Wuhan were presented as  
160 three-dimensional plots in **Figure 4**, compared with a reference value of 0 °C. The plots showed  
161 significant effect on COVID-19 incidence of temperature. In mainland China (outside of Hubei  
162 Province), the highest RR (1.71, 95% CI: 1.28-2.27) was observed at a cold temperature (-6 °C),  
163 suggesting the COVID-19 incidence were most likely to increase at -6 °C. The RR of 0.59 (95% CI:  
164 0.44-0.78) at 6 °C rose to 1.06 (95% CI: 0.96-1.18) when temperature dropped to -6 °C. However, no  
165 statistical significance was found in lag-specific relative risk at lag 2 to lag 4, suggesting no delayed  
166 effect at any temperature. For example, the relative risk maintained at lag 2-4, as lag-specific RR was  
167 1.14 (95% CI: 0.90-1.44) at lag 2 and 1.03 (95% CI: 0.86-1.33) at lag 4 when temperature was -6 °C. In  
168 Hubei Province (outside of Wuhan), RR was significantly higher at 8°C (RR 1.22, 95% CI: 1.07-1.38)  
169 and 10 °C (RR 1.92, 95% CI: 1.21-3.03) in lag 0. Conversely, lag-specific RR ranged from lag 0 to lag  
170 7 at 8-10 °C, suggesting positive delayed effect on decreasing COVID-19 incidence during the  
171 condition. In Wuhan city, the highest RR 1.04 (95% CI: 0.92-1.17) without significance was observed  
172 at approximately 9 °C. However, the incidence was more likely to decrease with immediate and  
173 delayed effect at a lower or higher temperature than 9 °C. For example, RR was in a range of 0.64 (95%  
174 CI: 0.46-0.87) to 0.88 (95% CI: 0.73-0.99) at lag 0 to 5 days when the temperature was 4 °C and  
175 similar results were observed when the temperature was 16 °C.

176 Overall pictures of the effect of absolute humidity on incidence in mainland China (outside of  
177 Hubei Province), Hubei Province (outside of Wuhan) and Wuhan were presented in **Figure 4**, showing  
178 3-D graphs of COVID-19 relative risk (RR) along absolute humidity and lags compared with a  
179 reference value of 7.5 g/m<sup>3</sup>. The plots showed inconsistent effect of absolute humidity on COVID-19  
180 incidence. In mainland China, immediate effect on COVID-19 incidence was strongest at absolute

181 humidity of  $4 \text{ g/m}^3$  (RR: 1.13, 95% CI: 1.02-1.27), indicating COVID-19 incidence was more likely to  
182 increase during the condition. When absolute humidity rose to  $5 \text{ g/m}^3$ , values of lag-specific RR were  
183 in range of 0.60 (95% CI: 0.36-0.99) to 0.62 (95% CI: 0.41-0.93) at lag 3 to lag 5 (**Supplementary**  
184 **Figure 3**), indicating a strong delayed effect on COVID-19 incidence at absolute humidity of  $5 \text{ g/m}^3$ . In  
185 Hubei Province, immediate effect on reducing COVID-19 incidence was observed when absolute  
186 humidity ranged from  $4.5 \text{ g/m}^3$  (RR 0.40, 95% CI: 0.19-0.84) to  $5.5 \text{ g/m}^3$  (RR 0.65, 95% CI: 0.44-0.96)  
187 (**Supplementary Figure 4**). However, no significant difference was observed in absolute humidity in  
188 Wuhan city (**Supplementary Figure 5**).

189       Considering the environmental impacts, we constructed the M-SEIR model to simulate the  
190 dynamic of COVID-19 by using the system dynamic section in AnyLogic software. SEIR dynamic  
191 transmission model compartmentalized the population into four states including susceptible, exposed,  
192 infected, and recovered, and further analyzed the relationships and interconnection using stock and set  
193 parameters, flows and table function (**Figure 5A; Supplemental video 1**). We set the initial values of  
194 the parameter and incorporated the temperature index in Wuhan city from Jan 20 and Feb 29, 2020,  
195 into the modified SEIR model. **Supplemental table 3** presented the comparison of modified SEIR  
196 model in our study and classic SEIR models in similar studies. The four curves were stratified by types  
197 of state, and showed a similar pattern: the population size increased early in epidemic and then  
198 decreased as the period ends (e.g., due to recovery). As the M-SEIR model predicted, the number of  
199 infections would peak around Mar 5, reaching the inflection point, and the COVID-19 outbreak in  
200 Wuhan would be expected to end by late April (**Figure 5B; Supplemental video 1**). Furthermore, a  
201 sensitivity analysis on the transmission rate adjusted by temperature indicated high stability of our  
202 M-SEIR model (**Figure 5C; Supplemental video 2**). We set the transmission rate from 0 to 1 with a

203 step of to 0.1, and conducted the simulations to reduce the bias involving in the model, parameters, and  
204 functional relationships. Finally, we found that the transmission rate decreased with the increase of  
205 temperature, leading to the decrease of infection rate and outbreak size.

206

## 207 **DISCUSSION**

208 We inferred that the number of new confirm COVID-19 cases in mainland China peaked on Feb 1,  
209 2020. COVID-19 daily incidence were lowest at -10 °C and highest at 10 °C, while the maximum  
210 incidence was observed at the absolute humidity of approximately 7 g/m<sup>3</sup>. We found significant  
211 association between temperature and COVID-19 daily incidence due to the immediate and delayed  
212 effect observed using DLNMs. As predicted in M-SEIR model, the COVID-19 outbreak would peak  
213 around March 5, 2020 and end in late April in Wuhan. Additionally, we found that transmission rate  
214 decreased with the increase of temperature, leading to further decrease of infection rate and outbreak  
215 size. Therefore, temperature drive the space and time correlations of COVID-19, and it can be used as  
216 an optimal predictor.

217 In this study, we inferred the significant association between temperature and COVID-19 daily  
218 incidence using LOESS, DLNMs and M-SEIR model, suggesting that temperature plays an important  
219 role in the outbreak of COVID-19 and can be used in predicting the potential spread of COVID-19.  
220 Lower and higher temperatures may be positive to decrease the COVID-19 incidence, which help to  
221 shed new light on the environmental drivers of COVID-19 in China. Our results are in line with the  
222 findings in SARS. Based on data on SARS and climate in 4 cities, Tan et al. found that temperature is a  
223 powerful indicator for SARS-CoV transmission, in which the risk of increased daily incidence differed

224 between the effects of high and low temperatures.<sup>16</sup> Additionally, Lowen's laboratory work evidenced  
225 that temperature affect the virus spread of aerosol using a guinea pig model.<sup>17</sup> However, the  
226 temperature DLNM in Hubei Province, showed different patterns from those in mainland China and  
227 Wuhan city, as COVID-19 relative risk rose at a moderate temperature.

228 In our analysis, we failed to observe a significant relationship between absolute humidity and  
229 COVID-19 incidence based on the data of mainland China. However, absolute humidity has been  
230 reported as a strong correlation with influenza epidemic, due to the seasonal pattern that influences the  
231 multiplications and spread of influenza.<sup>9 18 19</sup> In another study on MERS, caused a lethality of more  
232 than 35%, confirmed that the activity of MERS-CoV in droplet or aerosol, decreases significantly as  
233 absolute humidity increases though the mechanism is not yet clear.<sup>20</sup> The difference between our study  
234 and previous finding may result from the fact that absolute humidity remained stable in a region during  
235 a very limited period. Additionally, rapid and strong actions taken by the government could biased our  
236 study. Despite of the negative consequence in our study, further studies on absolute humidity are  
237 required to perform.

238 Combination of infectious disease dynamics model and environmental patterns is required to  
239 better explain the relationship between environmental factors and infection.<sup>21</sup> Dynamic transmission  
240 model was usually performed to predict the genesis and development trend of infectious diseases as  
241 well as to evaluate the effect of intervention but few dynamic transmission models included  
242 environmental factors for the increasing uncertainty. However, to reveal the dynamic of an infectious  
243 disease, it would be much better to take account of environmental impact on the basis of dynamic  
244 transmission model.<sup>22 23</sup>

245 Environmental factors, characterized by lag effects and threshold effects, can target at two objects,  
246 host and virus, during infectious disease outbreak. On one hand, human activity patterns and immunity  
247 can be influenced by environmental factors. But the effect caused by environmental condition was  
248 limited during the COVID-19 outbreak, due to the absence of extreme weather and specific immunity  
249 for a newly emerging virus. On the other hand, environmental impacts on the SARS-CoV-2 are more  
250 significant than the host population because the transmission and virulence of the virus varies in  
251 different conditions. Finally, environmental impacts on transmission of virus should be characterized in  
252 the dynamic model, because infectiousness estimated in the traditional dynamic model is actually a  
253 confounding effect with environmental effect. It is necessary to take account of environmental issues  
254 on the basis of dynamic transmission model so that the impacts could be isolated and qualified. A  
255 dynamic model is not only compatible with the infectious disease transmission mode for virus itself,  
256 but also can be well coupled with surveillance data on environmental issues.<sup>24</sup> Consequently, we  
257 constructed a M-SEIR model to correct the potential deviation of temperature to simulate the dynamic  
258 epidemic of COVID-19. The M-SEIR model predicted that the outbreak would reach its peak reach an  
259 inflection point around March 5, 2020, which is consistent with the actual situation based on data  
260 released by the NHC.<sup>25-29</sup> And it is expected that the COVID-19 outbreak in Wuhan would end in late  
261 April. In addition, we conducted a sensitivity analysis on the temperature-adjusted transmission rate.  
262 Finally, we found transmission rate decreased with the increase of temperature, leading to further  
263 decrease of infection rate and epidemic size.

264 Our analysis is subject to limitations. First, the COVID-19 dynamics are determined by multiple  
265 factors, including virus, climate, socio-economic development, population mobility, population  
266 immunity, and urbanization. However, not all those factors were considered in this study. Second, the

267 parameters of M-SEIR models were optimized, based on the previous analysis which might be biased  
268 by the lack of official data and the adjustment of diagnostic criteria in the outbreak. Third, it's an  
269 ecological analysis in very short period so that we cannot avoid the bias caused by other ecological  
270 factors changed over time.

271

## 272 **Conclusions and public health implications**

273 Temperature is an environmental driver of the COVID-19 outbreak in China. Lower and higher  
274 temperatures might be positive to decrease the COVID-19 incidence. As predicted in M-SEIR model,  
275 the COVID-19 outbreak would peak around March 5, 2020 and end in late April in Wuhan.  
276 Modified-SEIR models help to better evaluate and identify national and international prevention and  
277 intervention targeted COVID-19. The COVID-19 outbreak would not last for a long period of time  
278 with the increase of temperature, but the scale of the outbreak would be influenced by the measures  
279 taken among countries.

280

281 **Contributions:** All authors contributed to the study concept and design. PS, HY, and XL wrote the  
282 paper. PS and YD collected the data. PS, YD and CZ analyzed the data. PS, HY, ST, WL, MH, and SX  
283 reviewed and revised the manuscript before submission. All authors approved the final submitted  
284 version.

285 **Funding:** The work was supported by the National Key Research and Development Program of China  
286 to Prof Shuhua Xi (2018YFC1801204). The funders had no role in design and conduct of the study;

287 collection, management, analysis, and interpretation of the data; preparation, review, and approval of  
288 the manuscript; or the decision to submit the manuscript for publication.

289 **Competing interests:** All authors have completed the ICMJE uniform disclosure form at  
290 [http://www.icmje.org/coi\\_disclosure.pdf](http://www.icmje.org/coi_disclosure.pdf) (available on request from the corresponding author) and  
291 declare: no support from any organization for the submitted work other than those described above; no  
292 financial relationships with any organizations that might have an interest in the submitted work in the  
293 previous three years; no other relationships or activities that could appear to have influenced the  
294 submitted work.

295 **Transparency declaration:** The manuscript's guarantor affirms that the manuscript is an honest,  
296 accurate, and transparent account of the study being reported; that no important aspects of the study  
297 have been omitted; and that any discrepancies from the study have been explained.

298 **Data sharing:** No additional data available.

299

## 300 **References**

301 1. Zi Yue Zu M, Meng Di Jiang M, Peng Peng Xu M, Wen Chen M, Qian Qian Ni P, Guang Ming Lu M,  
302 et al. Coronavirus Disease 2019 (COVID-19): A Perspective from China.  
303 doi:10.1148/radiol.2020200490

304 2. She J, Jiang J, Ye L, Hu L, Bai C, Song Y. 2019 novel coronavirus of pneumonia in Wuhan, China:  
305 emerging attack and management strategies. *Clin Transl Med* 2020;9(1):19.  
306 doi:10.1186/s40169-020-00271-z

- 307 3. Wu Z, McGoogan JM. Characteristics of and Important Lessons From the Coronavirus Disease 2019  
308 (COVID-19) Outbreak in China: Summary of a Report of 72314 Cases From the Chinese Center for  
309 Disease Control and Prevention. *JAMA* 2020. doi:10.1001/jama.2020.2648
- 310 4. Li Q, Guan X, Wu P, Wang X, Zhou L, Tong Y, et al. Early Transmission Dynamics in Wuhan, China,  
311 of Novel Coronavirus-Infected Pneumonia. *The New England journal of medicine* 2020.  
312 doi:10.1056/NEJMoa2001316
- 313 5. Bedford T, Riley S, Barr IG, Broor S, Chadha M, Cox NJ, et al. Global circulation patterns of seasonal  
314 influenza viruses vary with antigenic drift, *Nature*.2015. doi:10.1038/nature14460
- 315 6. Lemaitre J, Pasetto D, Perez-Saez J, Sciarra C, Wamala JF, Rinaldo A. Rainfall as a driver of  
316 epidemic cholera: Comparative model assessments of the effect of intra-seasonal precipitation events.  
317 *Acta Trop*. 2019;190:235–243. doi:10.1016/j.actatropica.2018.11.013
- 318 7. Sooryanarain H, Elankumaran S. Environmental role in influenza virus outbreaks. *Annu Rev Anim*  
319 *Biosci* 2015;3:347-73. doi:10.1146/annurev-animal-022114-111017
- 320 8. Tamerius JD, Shaman J, Alonso WJ, Bloom-Feshbach K, Uejio CK, Comrie A, et al. Environmental  
321 predictors of seasonal influenza epidemics across temperate and tropical climates. *PLoS Pathog*  
322 2013;9(3):e1003194. doi:10.1371/journal.ppat.1003194
- 323 9. Dalziel BD, Kissler S, Gog JR, Viboud C, Bjornstad ON, Metcalf C, et al. Urbanization and humidity  
324 shape the intensity of influenza epidemics in U.S. cities. *Science* 2018;362(6410):75-79.  
325 doi:10.1126/science.aat6030
- 326 10. Thai PQ, Choisy M, Duong TN, Thiem VD, Yen NT, Hien NT, et al. Seasonality of absolute humidity

327 explains seasonality of influenza-like illness in Vietnam. *Epidemics* 2015;13:65-73.

328 doi:10.1016/j.epidem.2015.06.002

329 11. Li Y, Huang X, Yu IT, Wong TW, Qian H. Role of air distribution in SARS transmission during the

330 largest nosocomial outbreak in Hong Kong. *Indoor Air* 2005;15(2):83-95.

331 doi:10.1111/j.1600-0668.2004.00317.x

332 12. Chanprasopchai P, Pongsumpun P, Tang IM. Effect of Rainfall for the Dynamical Transmission

333 Model of the Dengue Disease in Thailand. *Comput Math Methods Med* 2017;2017:2541862.

334 doi:10.1155/2017/2541862

335 13. Liu T, Zhu G, He J, Song T, Zhang M, Lin H, et al. Early rigorous control interventions can largely

336 reduce dengue outbreak magnitude: experience from Chaozhou, China. *BMC Public Health*

337 2017;18(1):90. doi:10.1186/s12889-017-4616-x

338 14. Niakan Kalhori SR, Ghazisaeedi M, Azizi R, Naserpour A. Studying the influence of mass media and

339 environmental factors on influenza virus transmission in the US Midwest. *Public Health* 2019;170:17-22.

340 doi:10.1016/j.puhe.2019.02.006

341 15. Tianzhi Wu, Xijin Ge, Guangchuang Yu, Erqiang Hu. Open-source analytics tools for studying the

342 COVID-19 coronavirus outbreak. *medRxiv*. doi:10.1101/2020.02.25.20027433

343 16. Tan J. An initial investigation of the association between the SARS outbreak and weather: with the

344 view of the environmental temperature and its variation. *Journal of Epidemiology & Community Health*

345 2005;59(3):186-192. doi:10.1136/jech.2004.020180

346 17. Lowen AC, Mubareka S, Steel J, Palese P. Influenza virus transmission is dependent on relative

- 347 humidity and temperature. *PLoS Pathog* 2007;3(10):1470-6. doi:10.1371/journal.ppat.0030151
- 348 18. Shaman J, Goldstein E, Lipsitch M. Absolute humidity and pandemic versus epidemic influenza. *Am*  
349 *J Epidemiol* 2011;173(2):127-35. doi:10.1093/aje/kwq347
- 350 19. Shoji M, Katayama K, Sano K. Absolute humidity as a deterministic factor affecting seasonal  
351 influenza epidemics in Japan. *Tohoku J Exp Med* 2011;224(4):251-6. doi:10.1620/tjem.224.251
- 352 20. van Doremalen N, Bushmaker T, Munster VJ. Stability of Middle East respiratory syndrome  
353 coronavirus (MERS-CoV) under different environmental conditions. *Euro Surveill* 2013;18(38).  
354 doi:10.2807/1560-7917.es2013.18.38.20590
- 355 21. He D, Ionides EL, King AA. Plug-and-play inference for disease dynamics: measles in large and  
356 small populations as a case study. *J R Soc Interface* 2010;7(43):271-83. doi:10.1098/rsif.2009.0151
- 357 22. Martinez PP, King AA, Yunus M, Faruque AS, Pascual M. Differential and enhanced response to  
358 climate forcing in diarrheal disease due to rotavirus across a megacity of the developing world. *Proc Natl*  
359 *Acad Sci U S A* 2016;113(15):4092-7. doi:10.1073/pnas.1518977113
- 360 23. Bakker KM, Martinez-Bakker ME, Helm B, Stevenson TJ. Digital epidemiology reveals global  
361 childhood disease seasonality and the effects of immunization. *Proc Natl Acad Sci U S A*  
362 2016;113(24):6689-94. doi:10.1073/pnas.1523941113
- 363 24. Pitzer VE, Viboud C, Alonso WJ, Wilcox T, Metcalf CJ, Steiner CA, et al. Environmental drivers of  
364 the spatiotemporal dynamics of respiratory syncytial virus in the United States. *PLoS Pathog*  
365 2015;11(1):e1004591. doi:10.1371/journal.ppat.1004591
- 366 25. Tang Z, Li X, Li H. Prediction of New Coronavirus Infection Based on a Modified SEIR Model.

367 *medRxiv* 2020:2020.03.03.20030858. doi:10.1101/2020.03.03.20030858

368 26. Shi P, Cao S, Feng P. SEIR Transmission dynamics model of 2019 nCoV coronavirus with  
369 considering the weak infectious ability and changes in latency duration. *medRxiv*  
370 2020:2020.02.16.20023655. doi:10.1101/2020.02.16.20023655

371 27. Pan J, Yao Y, Liu Z, Li M, Wang Y, Dong W, et al. Effectiveness of control strategies for Coronavirus  
372 Disease 2019: a SEIR dynamic modeling study. *medRxiv* 2020:2020.02.19.20025387.  
373 doi:10.1101/2020.02.19.20025387

374 28. Hong N, He J, Ma Y, Jiang H, Han L, Su L, et al. Evaluating the secondary transmission pattern and  
375 epidemic prediction of the COVID-19 in metropolitan areas of China. *medRxiv*  
376 2020:2020.03.06.20032177. doi:10.1101/2020.03.06.20032177

377 29. Zhang L, Wan K, Chen J, Lu C, Dong L, Wu Z. When will the battle against novel coronavirus end in  
378 Wuhan: a SEIR modeling analysis. *medRxiv* 2020:2020.02.16.20023804.  
379 doi:10.1101/2020.02.16.20023804

380

381 **Figure Legends**

382 **Figure 1** Daily number of new confirmed cases of COVID-19 in mainland China between Jan 20 and  
383 Feb 29, 2020.

384 **Figure 2** Between Jan 20 and Feb 29, 2020, temperature values (left columns) and absolute humidity  
385 values (right columns) in 31 provincial-level regions in mainland China.

386 **Figure 3** COVID-19 daily incidence indicators (daily incidence and  $\lg N$ ) and the expected values  
387 based on the temperature and absolute humidity in mainland China (outside of Hubei Province) from  
388 Jan 20 to Feb 29, respectively. The black line represents the expected value of a daily incidence and  
389  $\lg N$  based upon a LOESS regression for all days of available estimates. LOESS, locally weighted  
390 regression and smoothing scatterplots.

391 **Figure 4** 3-D plot of RR of COVID-19 along climate factors (temperature and absolute humidity) and  
392 lags in mainland China (outside of Hubei Province), Hubei Province (outside of Wuhan), and Wuhan  
393 city.

394 **Figure 5 COVID-19 dynamic trends and sensitivity analysis using M-SEIR model in Wuhan. (A)**

395 The over-all structure of M-SEIR model constructed by using the system dynamic section in AnyLogic  
396 software. **(B)** The snapshot represents the different population proportion of susceptible, exposed,

397 infected, and recovered states under the specific time-point and forecasts the trend of the COVID-19

398 outbreak in Wuhan city. **(C)** Sensitivity analysis under different temperature scenarios in Wuhan city.

399 As the temperature-corrected transmission index rises, the peak of the curve increased under different

400 times gradually. M-SEIR model, modified susceptible-exposed-infectious-recovered model; TI, the

401 temperature-corrected transmission index (i.e. The transmission rate for susceptible to exposed,  $\beta_t$ ).

## Figures

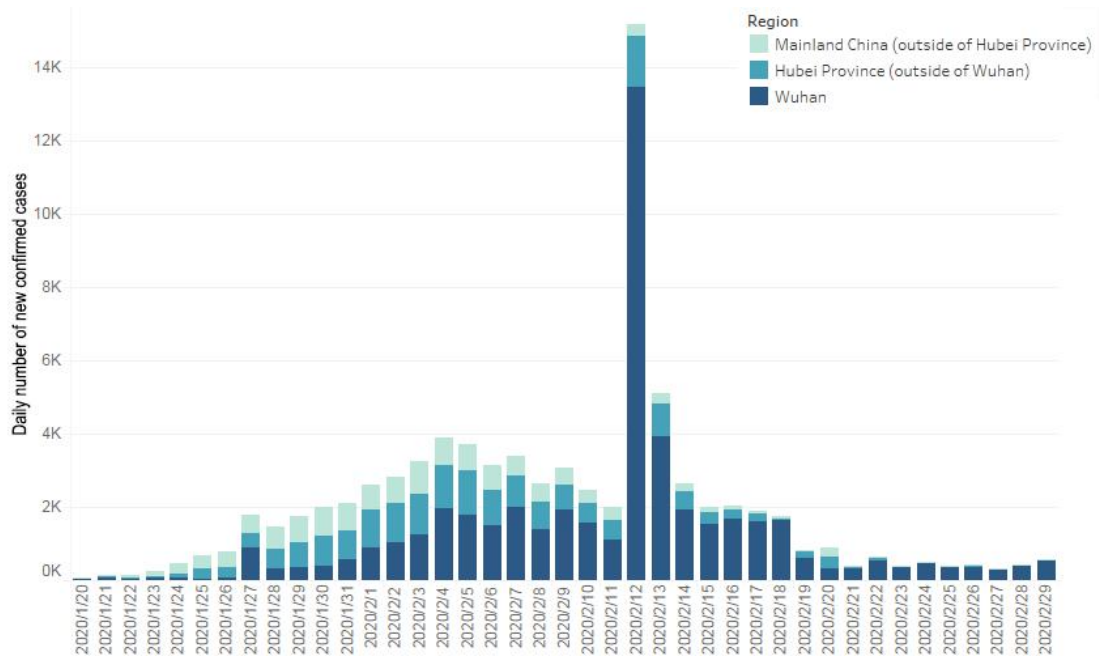


**Figure 1** Daily number of new confirmed cases of COVID-19 in mainland China between Jan 20 and

Feb 29, 2020.

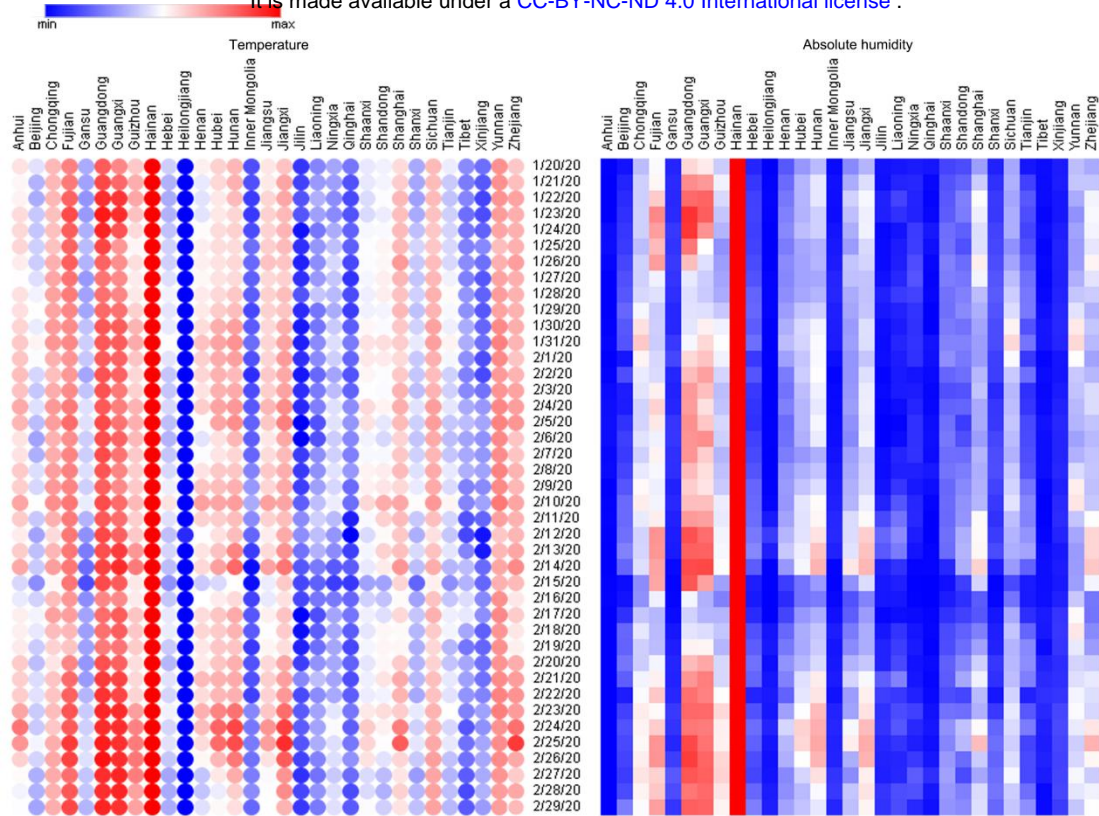


**Figure 2** Between Jan 20 and Feb 29, 2020, temperature values (left columns) and absolute humidity values (right columns) in 31 provincial-level regions in mainland China.

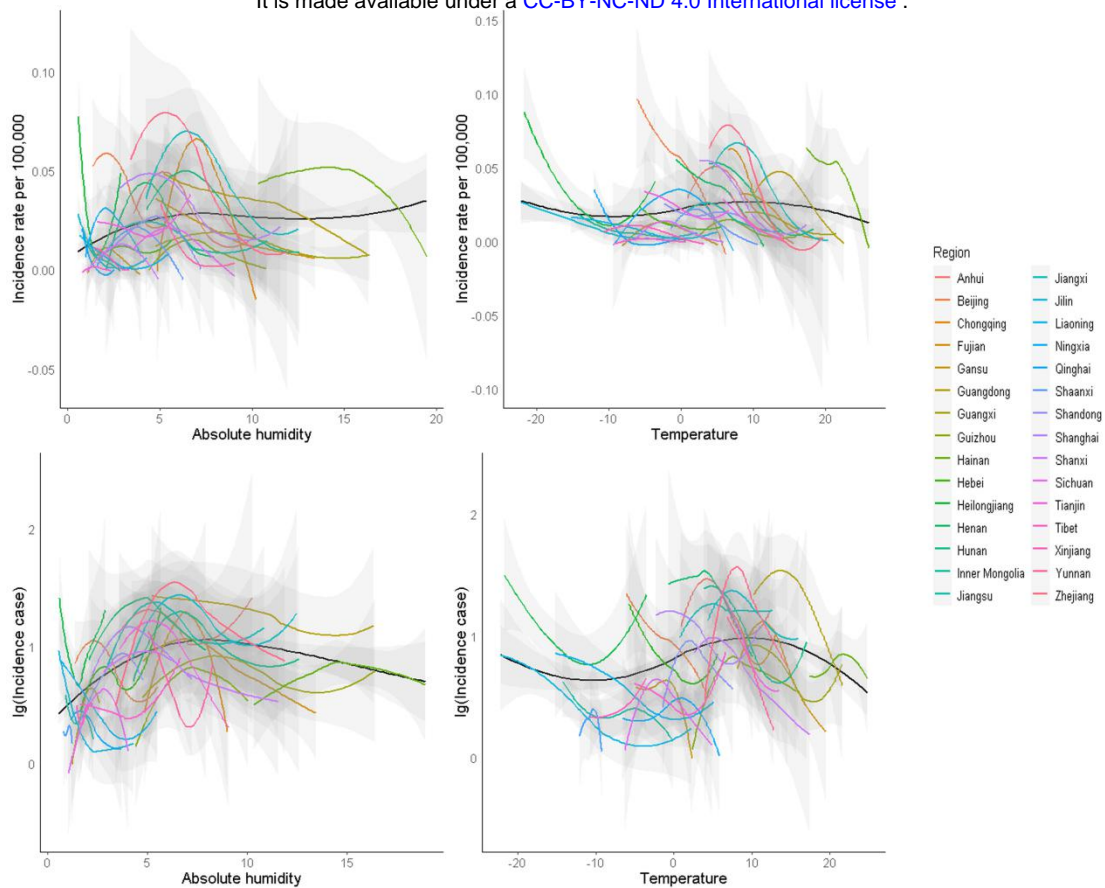


**Figure 3** COVID-19 daily incidence indicators (daily incidence and lgN) and the expected values based on the temperature and absolute humidity in mainland China (outside of Hubei Province) from Jan 20 to Feb 29, respectively. The black line represents the expected value of a daily incidence and lgN based upon a LOESS regression for all days of available estimates. LOESS, locally weighted regression and smoothing scatterplots.

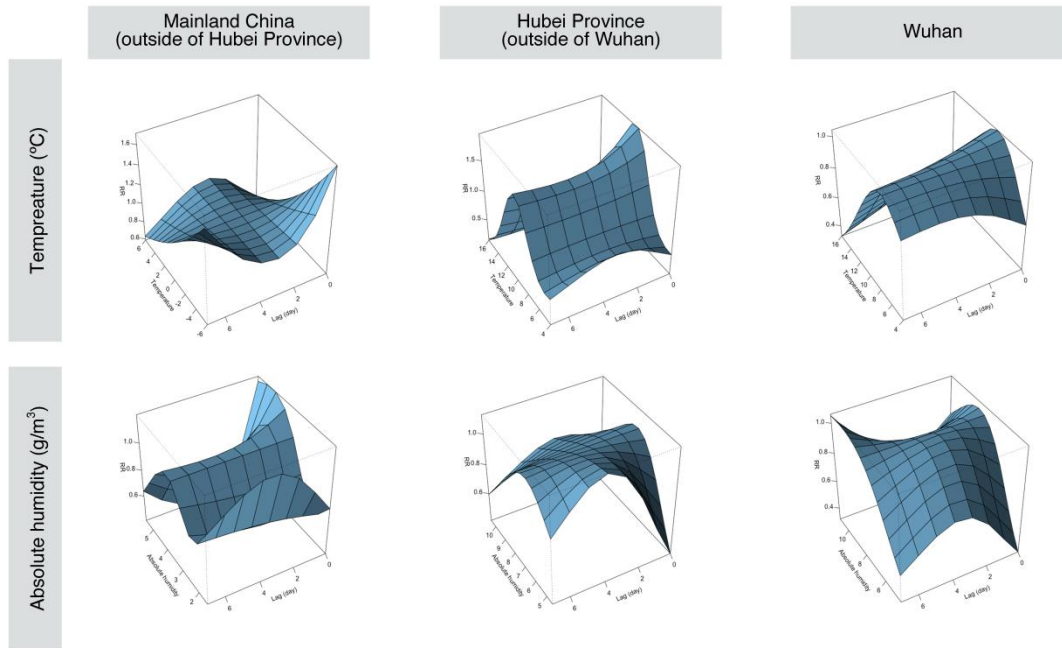


**Figure 4** 3-D plot of RR of COVID-19 along climate factors (temperature and absolute humidity) and lags in mainland China (outside of Hubei Province), Hubei Province (outside of Wuhan), and Wuhan city.

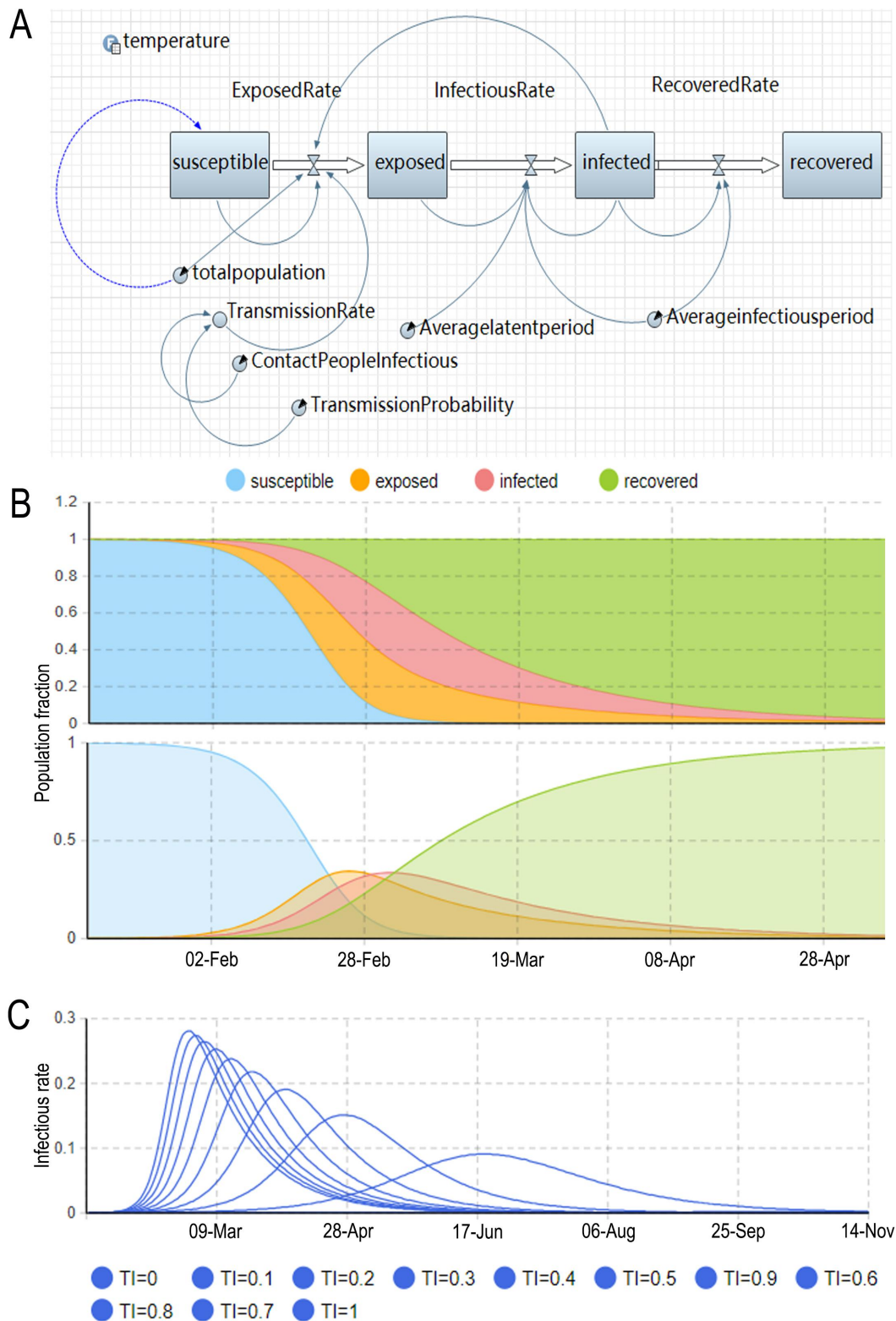


**Figure 5 COVID-19 dynamic trends and sensitivity analysis using M-SEIR model in Wuhan. (A)**

The over-all structure of M-SEIR model constructed by using the system dynamic section in AnyLogic software. **(B)** The snapshot represents the different population proportion of susceptible, exposed,

infected, and recovered states under the specific time-point and forecasts the trend of the COVID-19

outbreak in Wuhan city. (C) Sensitivity analysis under different temperature scenarios in Wuhan city.

As the temperature-corrected transmission index rises, the peak of the curve increased under different

times gradually. M-SEIR model, modified susceptible-exposed-infectious-recovered model; TI, the

temperature-corrected transmission index (i.e. The transmission rate for susceptible to exposed,  $\beta_t$ ).